Elsevier Editorial System(tm) for Food Hydrocolloids

Manuscript Draft

Manuscript Number: FOODHYD-D-12-00246R2

Title: Development of novel ultrathin structures based in amaranth (Amaranthus hypochondriacus) protein isolate through electrospinning

Article Type: Original Research Paper

Keywords: amaranth protein; electrospinning; encapsulation; ultrathin structures

Corresponding Author: Dr. Amparo Lopez-Rubio,

Corresponding Author's Institution: IATA-CSIC

First Author: Marysol Aceituno-Medina

Order of Authors: Marysol Aceituno-Medina; Amparo Lopez-Rubio; Sandra Mendoza; Jose M Lagaron

Abstract: Amaranth protein isolate (API) ultrathin structures have been developed using the electrospinning technique. The effects of pH, type of solvent and surfactant addition on the spinnability, morphology and molecular organization of the obtained structures have been studied. Regarding the effect of pH on API electrospinning, capsule morphologies were only obtained at extreme pH values (i.e. pH 2 and pH 12), which allowed the solubilisation of the proteins, and the process was favoured when the solutions were previously heated to induce protein denaturation. Fibre-like morphologies were only obtained when the solvent used for electrospinning was hexafluoro-2-propanol, as this organic solvent promotes the formation of random coil structures and, thus, an increase in the biopolymer entanglements.
Capsule morphologies were obtained from the API-containing formic acid solutions and this solvent was better for electrospraying than the acetic acid, probably due to the higher viscosity and lower surface tension of the solutions thereof. Addition of 20 wt.-% of Tween 80 considerably improved the formation of capsule-like structures from the formic acid solution, as this surfactant contributed to the formation of alpha helical structures. Similar results were obtained when combining the surfactant with the reducing agent 2-mercaptoethanol. However, denaturation of the protein structure was not sufficient for fibre formation through electrospinning, as the solution properties play a fundamental role in determining the morphology of the electrospun structures.

Development of novel ultrathin structures based in amaranth (*Amaranthus hypochondriacus*) protein isolate through electrospinning

Marysol Aceituno-Medina[1], Amparo Lopez-Rubio[2*], Sandra Mendoza[1], José María Lagaron[2]

[1] Departamento de Investigación y Posgrado en Alimentos, Facultad de Química, Universidad Autónoma de Querétaro, Cerro de las Campanas s/n, Querétaro, Qro., 76010, México.

[2] Novel Materials and Nanotechnology Group, IATA-CSIC, Avda. Agustin Escardino 7, 46980 Paterna (Valencia), Spain

*Corresponding author: Tel.: +34 963900022; fax: +34 963636301

E-mail address: amparo.lopez@iata.csic.es (A. López-Rubio)

Abstract

Amaranth protein isolate (API) ultrathin structures have been developed using the electrospinning technique. The effects of pH, type of solvent and surfactant addition on the spinnability, morphology and molecular organization of the obtained structures have been studied. Regarding the effect of pH on API electrospinning, capsule morphologies were only obtained at extreme pH values (i.e. pH 2 and pH 12), which allowed the solubilisation of the proteins, and the process was favoured when the solutions were previously heated to induce protein denaturation. Fibre-like morphologies were only obtained when the solvent used for electrospinning was hexafluoro-2-propanol, as this organic solvent promotes the formation of random coil structures and, thus, an increase in the biopolymer entanglements. Capsule morphologies were obtained from the API-containing formic acid solutions and this solvent was better for electrospraying than the acetic acid, probably due to the higher viscosity and lower surface tension of the solutions thereof. Addition of 20 wt.-% of Tween 80 considerably improved the formation of capsule-like structures from the formic acid solution, as this surfactant contributed to the formation of alpha helical structures. Similar results were obtained when combining the surfactant with the reducing agent 2-mercaptoethanol. However, denaturation of the protein structure was not sufficient for fibre formation through electrospinning, as the solution properties play a fundamental role in determining the morphology of the electrospun structures.

Keywords: amaranth protein, electrospinning, encapsulation, ultrathin structures

1. Introduction

The development of ultrathin and/or nanofibres from biodegradable and biocompatible synthetic and natural polymers through the electrospinning technique has boosted the interest in areas of biomedicine, pharmaceuticals, cosmetics and, more recently, in the food industry due to their potential applications, amongst others, as high-performance encapsulation systems for bioactive compounds (Lopez-Rubio & Lagaron, 2012; Torres-Giner, Martinez-Abad, Ocio, & Lagaron, 2010). Electrospinning is a process that produces continuous polymer fibres with diameters in the submicrometer range through the action of an external electric field imposed on a polymeric solution or melt (Reneker & Chun, 1996). In the food science area, this technique has recently been applied to encapsulate antioxidants (Li, Lim, & Kakuda, 2009; Lopez-Rubio & Lagaron, 2012; Torres-Giner et al., 2010) and probiotic bacteria (Heunis, Botes, & Dicks, 2010; Lopez-Rubio, Sanchez, Sanz, & Lagaron, 2009; Lopez-Rubio, Sanchez, Wilkanowicz, Sanz, & Lagaron, 2012), demonstrating the great potential of electrospinning as a versatile micro- submicro- and nanoencapsulation processing technique to generate ingredients for functional food products. The morphology of the structures obtained through electrospinning can be varied by adjusting the process parameters and, for a certain material, small capsules can be obtained when lowering the polymer concentration and/or increasing the tip-to-collector distance. In this case, the electrospinning process is normally referred to as "electrospraying" due to the non-continuous nature of the structures obtained. The main factors that influence the morphology of the electrospun structures are the solution properties (specifically the viscosity, conductivity and surface tension of the polymer solutions) and the process parameters (mainly voltage, distance to collector, flow rate and ambient humidity) (Chakraborty, Liao, Adler, & Leong, 2009). The solution properties are

defined by the polymer type, molecular weight and concentration as well as by the solvent properties. It is generally considered that for fibre development, a critical chain entanglement is needed which usually requires a certain viscosity of the solutions and avoiding too high surface tension values. The size of the fibres of capsules generated can be modified by changing the previous mentioned parameters and, for instance, increasing the polymer concentration and reducing the surface tension or the distance to the collector, leads to greater fibre or capsule diameters (Chakraborty et al., 2009).

There is a wide range of polymers which can be used to entrap, coat or encapsulate substances of different types, origins and properties. Recently, the interest to develop functional matrices using natural substances such as proteins, carbohydrates and lipids have increased due to consumer awareness of the environmental damage caused by non-biodegradable materials and health issues. These materials come from renewable resources and they may be nontoxic, edible, and digestible. The importance to develop biodegradable materials is not only focused on food applications, but also on the potential to create a completely new market for commodities or wastes arising from agricultural production. In this context, amaranth (*Amaranthus hypochondriacus*) is a traditional Mexican plant that remains as an underutilized crop which provides both grains and tasty leaves of high nutritional value (Silva-Sánchez *et al.,* 2008). The seed has high protein content (17%), and its amino acid composition is close to the optimum amino acid balance required for the human diet (Schnetzler & Breen, 1994; Teutónico & Knorr, 1985). Contrarily to most common grains, the proteins in amaranth are mainly composed of globulins and albumins, and contain very little or no storage prolamin proteins, which are the main storage proteins in cereals, and also the toxic proteins in celiac disease (Drzewiecki *et al.,* 2003; Gorinstein *et al.,* 2002). Several studies suggest that grain amaranth derivatives represent interesting

ingredients for food formulations and promissory materials for the development of edible and/or biodegradable films (Colla, Sobral, & Menegalli, 2006; Elizondo, Sobral, & Menegalli, 2009; Tapia-Blácido, Mauri, Menegalli, & Sobral, 2005). However, to the best of our knowledge, to date there is neither published information about the development of encapsulation systems (nano- or microstructures) based in amaranth protein nor about the processing of this protein by electrospinning.

The main objective of this research work was to evaluate the feasibility of producing electrospun structures (fibres and/or beads) from amaranth protein isolate (API) and to evaluate the influence of pH, temperature and the use of different solvents and co-spinning agents (various surfactants and a reducing agent) on the morphology and molecular organization of the electro-deposited material. These structures are envisaged as potential novel fabrication processing morphologies and textures for the protein or as bioactive encapsulation matrices for functional food applications.

2. Experimental part

2.1 Materials

Glacial acetic acid of 99.7% purity and sodium hydroxide pellets of 98% purity were supplied by Panreac (Barcelona, Spain). Formic acid of 95% purity, 1,1,1,3,3,3-hexafluoro-2-propanol (HFIP), 2-mercaptoethanol (2-ME), non-ionic surfactant, polyoxyethylene sorbitan monooleate (Tween 80) and amphoteric surfactant, L-α-phosphatidylcholine were supplied by Sigma-Aldrich. The anionic surfactant, sodium stearoyl lactate (SSL) was supplied by Danisco and a commercial amaranth protein concentrate (*Amaranthus hypochondriacus* L. Revancha variety) was supplied by Nutrisol (Hidalgo, Mexico).

2.2 Preparation of amaranth protein isolate (API)

The amaranth protein isolate (API) used in this study was prepared according to Martínez and Añón (1996). Briefly, the commercial amaranth protein concentrate (APC) was defatted with hexane for 12 h (10% w/v suspension). Then, the amaranth protein concentrate was suspended in water and its pH was adjusted to 9 with a 2 N NaOH solution. The suspension was stirred for 30 min at room temperature and, then, centrifuged 20 min at 9000 *g*. Then, the supernatant was adjusted to pH 5 with 2 N HCl and centrifuged at 9000 g for 20 min at 4°C. The pellet was resuspended in water, neutralized with 0.1 N NaOH and freeze-dried. The protein content was determined by the Kjeldahl technique (AOAC 1996) using a conversion factor of 5.85.

2.3 Determination of API molecular weight by gel electrophoresis

The amaranth protein isolate was characterized based on its protein profile using sodium dodecyl sulfate-polyacrylamide gel electrophoresis (SDS-PAGE). The runs were carried out in the following continuous buffer system: 0.5M Tris-HCl pH 6.8/1% (w/v) SDS for the stacking gel, and 1.5M Tris-HCl 8.8/1% (w/v) SDS for the separating gel. The stacking and separating gels were prepared with 4% and 15% (w/v) acrylamide, respectively. Protein samples (10 mg/mL) were dissolved in 0.5 M Tris-HCl, pH 6.8/8% (v/v) glycerol/1% (w/v) SDS/0.05% (w/v) bromophenol blue and centrifuged at 15800*g* for 5 min; the supernatants (32 µl) were used to load the gel. For runs in reducing conditions the sample buffer contained 5% 2-ME and samples were heated for 1 min in a boiling-water bath. The standard molecular weight proteins (Mark 12^{TM} unstained standard) were supplied by Invitrogen. After electrophoresis, the gel was fixed with trichloroacetic acid (12.5% w/v) for 30 min and stained overnight by addition of Coomassie Brilliant Blue.

2.4 Preparation of polymer solutions for electrospinning

The preparation of the different solutions for electrospinning is described below:

2.4.1 Amaranth protein isolate aqueous solutions at different pH values.

Aqueous solutions containing either 1N of glacial acetic acid or 0.01M of NaOH of amaranth protein isolate (5, 10, 12 and 15% w/w) were prepared at different pH values (ranging from 2 to 12) with and without heating (80°C/30 minutes). Before electrospinning, the solutions were stirred until the protein was completely dissolved.

2.4.2 Use of other solvents for the preparation of fibre-forming solutions

Apart from the acetic acid and sodium hydroxide aqueous solutions, two other solvents were tested for dissolving and electrospinning the amaranth protein isolate: HFIP, and formic acid.

HFIP solution. Fibre-forming solutions were prepared by dissolving different concentrations of amaranth protein (5, 8, 10 % w/w) in HFIP at 25ºC under magnetic stirring until the protein was completely dissolved. The pH of these solutions was around 6.

Formic acid solution. Solutions were prepared by dissolving different concentrations of amaranth protein (8, 10, 20 % w/w) in formic acid at 25ºC under magnetic stirring until the protein was completely dissolved. The pH of these solutions was around 2.

2.4.3 Effects of different surfactants and a reducing agent on the preparation of fibre-forming solutions

Tween 80, Sodium stearoyl lactate (SSL), L-α-phosphatidylcholine, and 2-mercaptoethanol were incorporated in 10, 15, 20, 25% w/w with respect to the weight of the protein in the solution. Each solution was stirred for 1 hour at room temperature before electrospinning.

2.5 Characterization of the polymeric solutions

The viscosity of the polymeric solutions was determined using a rotational viscosity meter Visco Basic Plus L from Fungilab S.A. (San Feliu de Llobregat, Spain) using a Low Viscosity Adapter (LCP). The surface tension of the polymer solutions was measured using the Wilhemy plate method in a EasyDyne K20 tensiometer (Krüss GmbH, Hamburg, Germany). Both tests were carried out in triplicate. The conductivity of the solutions was measured using a conductivity meter XS Con6 (Labbox, Barcelona, Spain). The pH values were measured using a multi-parameter analyzer CONSORT C380 from Biotech (Madrid, Spain). All measurements were made at 25ºC.

2.6 Electrospinning technique

The electrospinning apparatus, a FluidNatek® instrument, trademark of the engineering division of BioInicia S.L. (Valencia, Spain), equipped with a variable high voltage 0–30 kV power supply was used. The anode was attached to a stainless-steel needle with internal diameter 0.9 mm that was connected through a PTFE tubing to the biopolymer solutions kept in a 5 ml plastic syringe. The syringe was disposed horizontally lying on a digitally controlled syringe pump while the needle was vertically directed towards the collector. The needle was connected to the emitting electrode of positive polarity of the high voltage power supply. A positively charged jet of the polymer solution was formed from the Taylor cone that travelled through the air gap and was deposited on the collector. The proprietary amaranth-based electrospun structures (P201131705 Patent Application, 2011) were collected on an aluminum foil sheet attached to a copper grid used as collector. All of the electrospinning experiments were carried out at room temperature in air. The electrospinning environmental conditions were maintained stable at 24°C and 60% RH by

185 having the equipment enclosed in a specific chamber with temperature and humidity
186 control. The electrospinning conditions of voltage, tip to collector distance and feed rate
187 were fixed at 14 kV, 10 cm and 0.3 ml/h, respectively.
188
189 **2.7 Scanning Electron Microscopy (SEM)**
190 The morphology of the electrospun fibres was examined using SEM (Hitachi S-4100) after
191 sputtering the samples with a gold–palladium mixture under vacuum. All SEM experiments
192 were carried out at an accelerating voltage of 10 kV. The diameters of the electrospun
193 structures were measured by means of the Adobe Photoshop 7.0 software from the SEM
194 micrographs in their original magnification. At least, 50 electrospun structures from each
195 sample, were considered to obtain the average diameter.
196
197 **2.8 Optical microscopy**
198 Optical microscopy images were taken using a digital microscopy system (Nikon Eclipse
199 90i) fitted with a 12 V, 100 W halogen lamp and equipped with a digital imaging head. Nis
200 Elements software (Nikon Instruments Inc., Melville, USA) was used for image capturing
201 and the Adobe Photoshop 7.0 software was used for image processing and analysis.
202
203 **2.9 Attenuated total reflectance infrared spectroscopy (ATR-FTIR)**
204 ATR-FTIR spectra were collected in a controlled chamber at 24°C and 40% RH coupling
205 the ATR accessory GoldenGate of Specac Ltd. (Orpington, UK) to a Bruker (Rheinstetten,
206 Germany) FTIR Tensor 37 equipment. All the spectra were collected by averaging 20 scans
207 at 4 cm^{-1} resolution. Analysis of the spectral data was performed using Grams/AI 7.02
208 (Galactic Industries, Salem, NH, USA) software.

209

210 **2.10 Statistical analysis**

211 One-way analysis of the variance (ANOVA) was performed using XLSTAT-Pro (Win)
212 7.5.3 (Addinsoft, NY) software package. Comparisons between samples were evaluated
213 using the Tukey test ($\alpha = 0.05$).

214

215

3. Results and discussions.

3.1 Characterization of amaranth protein isolate (API)

The protein content of amaranth protein concentrate (APC) obtained commercially was 30.9 ± 0.4%. After the purification carried out, the amaranth protein isolate (API) obtained had a protein content of 85.5 ± 0.2%. Similar protein contents for API were obtained by Abugoch, Martínez, & Añón (2010) (84.4%) and Martínez & Añón (1996) (80-90%) using the same isolation procedure. According to the results obtained by electrophoresis (cf. Figure 1), the amaranth protein isolate consisted of a mixture of different proteins with molecular weights ranging from ~10 to ~83 kDa. These results are in agreement with the values obtained by other authors (Abugoch *et al.,* 2010; Martínez & Añón, 1996; Marcone, 1999).

INSERT FIGURE 1 ABOUT HERE

3.2 Effect of pH and temperature on the morphology and molecular organization of electrospun API

Initially, the solubility of API at different pH values (ranging from 2 to 12) was investigated. From previous works it is known that the solubility profile of amaranth proteins at various pH values is characterized by a solubility minimum around the mean isoelectric point (between 4.5 and 6.5) reported for different amaranth protein fractions (Konishi, Horikawa, Oku, Azumaya, & Nakatani, 1991), because protein-protein interactions increase as the net electrostatic charges of the molecules are at a minimum and less water interacts with the protein molecules (Salcedo-Chávez, Osuna-Castro, Guevara-

240 Lara, Domínguez-Domínguez, & Paredes-López, 2002). A moderate and high solubility
241 was only obtained at pH 2 and 12, respectively. Consequently, different concentrations of
242 the protein (5, 10, 12 and 15% w/w) were tested at both pH conditions using aqueous
243 solutions containing either acetic acid 1N for pH 2 or sodium hydroxide for pH 12 (0.01M).
244 In the case of the acid solution, protein concentrations greater than 5% w/w, led to the
245 development of a strong gel after 15 minutes of agitation. This could be explained by the
246 formation of hydrogen bonds between the acetic acid solution and the protein amino acids,
247 which induces the polymer chains to arrange in α-helical and β-sheet configurations, both
248 leading to the gelling of the solution (Van der Leeden, Rutten, & Frens, 2000).
249 On the other hand, due to the greater solubility of API in the alkaline solution, it was
250 possible to incorporate up to 15 wt.-% of the protein without gel formation. Both systems,
251 acid and alkaline, were subjected to the electrospinning process. Figure 2 shows SEM
252 images of the structures obtained. Despite systematic variations of applied voltage (10-22
253 kV) and tip-to-collector distance (6-25 cm) no fibre was obtained, but instead, a few
254 capsules together with amorphous material were collected (cf. Figure 2). Amaranth protein
255 isolates are mainly composed by albumins and globulins (Quiroga, Martínez, & Añón,
256 2007; Scilingo, Molina, Martínez, & Añón, 2002), which have a globular structure and
257 their polyelectrolytic character give rise to a multitude of inter- and intramolecular
258 interactions. These characteristics, specifically the strong molecular interactions,
259 complicate the formation of fibre structures. The above-mentioned α-helical and β-sheet
260 polymer chain configurations which may be adopted in the acetic acid solution also keep
261 the rigidity of the chains, preventing the formation of fibres through electrospinning.
262 Table 1 summarizes the morphology and diameters of the structures obtained from API in
263 acetic acid and sodium hydroxide solutions after the electrospinning process. In this table,

264 solution properties (viscosity, conductivity and surface tension) are also included. Failure to
265 obtain electrospun fibres from pure biopolymer dispersions has been previously reported
266 and it is usually an indication of low viscosity and lack of sufficient entanglement (Buchko,
267 Chen, Shen, & Martin, 1999; Wongsasulak, Kit, Mcclements, Yoovidhya, & Weiss, 2007;
268 Wongsasulak, Patapeejumruswong, Weiss, Supaphol, & Yoovidhya, 2010).
269
270
271 INSERT TABLE 1 ABOUT HERE
272
273 The application of heat can help to facilitate denaturation of the proteins, leading to an
274 unfolded state and minimizing the inter- and intra-molecular interactions. Consequently, the
275 developed solutions at the extreme pH conditions, i.e. the one with acetic acid (pH 2, 5%
276 w/w API) and the alkaline solution (pH 12, 15% w/w API), were heated to 80°C, in order
277 to study the influence of heating on the morphology of the electrospun structures. Although
278 temperature did not led to fibre-like morphologies, it facilitated the formation of
279 microparticles or capsules which were deposited on the collector plate from these solutions,
280 probably due to the increased viscosity of the denatured solutions (see Table 1). Some
281 morphological changes could be appreciated between the obtained electrosprayed structures
282 and, while dented droplets were obtained from the acid solution, smooth and round
283 capsules were formed from the heated alkaline one. However, the acid solutions seemed to
284 be more efficient for capsule development, as deduced from the collected electrosprayed
285 material (cf. Figure 2). The greater facility for capsule development of the API acid
286 solution may be related to the higher viscosity and lower surface tension of this solution,
287 while the greater average capsule size can be explained by its lower conductivity (cf. Table

1). On the other hand, because of the oligomeric structure of API proteins, it is possible that high alkaline environments (pH 12) induce their dissociation, thus increasing low molecular weight species (Konishi, Fumita, Ikeda, Okuno, & Fuwa, 1985; Marcone, 1999; Rajendran & Prakash, 1988). This process causes a drop of the viscosity, consequently preventing the electrospinning process (cf. Table 1 and Figure 2). Similar results have been reported by Torres-Giner and co-workers (2008) with alkaline solutions of zein.

However, it is worth mentioning that given the dynamic nature of the electrospinning process, the static values obtained for the conductivity, surface tension and viscosity may only serve as a guide. Moreover, working with biopolymers can be challenging, not only due to the property variations depending on source, extraction method and handling procedures, but also due to potential solution property changes with time (Schiffman & Schauer, 2008). It is also known that the rheological behaviour of the solution (specifically the viscoelasticity), more than its viscosity, plays an important role during electrospinning.

INSERT FIGURE 2 ABOUT HERE

The infrared spectra of electrosprayed structures obtained using acid acetic as a solvent is shown in Fig. 3. Characteristic peaks for the amaranth protein isolate (API) were identified at ~1634 cm^{-1} and 1533 cm^{-1}, which correspond to the amide I and II regions respectively. The absorption peak at ~1634 cm^{-1} can be attributed to the stretching of the C=O (Amide I) while the peak at 1533 cm^{-1} is due to stretching of C-N and bending of N-H (Amide II). Amide I band has been widely used to study protein folding, unfolding and aggregation with infrared spectroscopy due to its sensitivity to secondary structure of proteins. The spectrum of the API powder (cf. spectrum B in Figure 3) shows bands at 1634 (strong) and

1692 cm^{-1} (weak), which are characteristic of β-sheet structures. After electrospinning, the amide I band considerably broadens indicating a greater conformational freedom of the protein chains (Barth, 2007). A previous study with amaranth protein isolates at different pH conditions showed higher quantity of random coils and less structured domains at pH 2 (Ventureira et al., 2012), thus confirming the results shown here. Moreover, apart from the broadening, another maximum centred near 1650 cm^{-1} is clearly seen for the electrosprayed API structures, which is characteristic of α-helices and unfolded proteins (Barth, 2007). Some residual solvent remained in the electrosprayed structures as observed in the infrared spectrum, which was almost eliminated after drying at 60ºC during 30 minutes (see arrows in spectra C and D of Figure 3). Comparing these two spectra it is also apparent that upon elimination of the acetic acid, the contribution of the β-sheet configuration to the secondary structure of the protein was clearly diminished (see dotted line in Figure 3 indicating the position of the band related to the β-sheet configuration), which is consistent with a less structured arrangement of the protein chains.

INSERT FIGURE 3 ABOUT HERE

Regarding the electrospun structures obtained from the basic solution, no significant spectral differences were observed when compared with the API spectrum (results not shown), just a slight shift of the amide I band from 1634 to 1638 cm^{-1} which may indicate a relaxation of the hydrogen bonds from the secondary structure of the proteins (Barth, 2007).

3.3 Effect of the type of solvent used during electrospinning

The type of solvent and the physical properties (viscosity, surface tension and conductivity) of the solutions are important parameters in the electrospinning process. In a poor solvent, which is energetically unfavourable, the dissolution of the polymer is an endothermic process and the polymer segments will be attracted to one another in the solution and squeeze out the solvent between them. The polymer chains will adopt a curled configuration with increased polymer-polymer interactions, fact that can lead to gelation. Moreover, the configuration that is adopted by the polymer chains in solution, will affect its intrinsic viscosity. An extended or uncurled configuration of the polymer chain molecules is associated with an increase in the intrinsic viscosity of the solution, while polymer chains that adopt a curled configuration in the solvent will result in an intrinsic viscosity drop. An extended or uncurled configuration of the polymer chains in solution is necessary for fibre formation during electrospinning (Ramakrishna, Fujihara, Teo, Lim, & Ma, 2005).

Apart from the acid and basic aqueous solutions mentioned in the previous paragraphs, and with the aim of improving the spinnability of API, two other solvents were evaluated: Hexafluoroisopropanol (HFIP) and formic acid.

According to the literature, HFIP is a highly versatile and volatile solvent that has been widely used due to its ability to dissolve nylons and proteins and because it provides solutions with excellent physical properties for electrospinning applications (Li, McCann, & Xia, 2005; Matthews, Wnek, Simpson, & Bowling, 2002; Woerdeman *et al.*, 2005). Different protein concentrations (5, 8 and 10% w/w) in HFIP were tested and the morphologies of the obtained electrospun structures are shown in Figure 4.

INSERT FIGURE 4 ABOUT HERE

Concentrations of 5% w/w formed beaded fibres, while concentrations of 8% w/w of protein formed flat fibres. Some fibres were also formed from the solution containing 10 wt.-% API, but the high viscosity of the same, prevented a stable ejection of a polymer jet from the tip of the syringe. The morphology of the obtained fibres was similar to the one obtained from wheat proteins using the same solvent (Woerdeman *et al.,* 2005). HFIP is a solvent that allows an increase in the percentage of random coil structures, which causes an increase in the hydrodynamic volume and the degree of biopolymer entanglement in solution (Dror *et al*., 2008; Gupta, Eelkins, Long, & Wilkes, 2005; Hirota, Mizuno, & Goto, 1997). The increase in random coil structures was confirmed by means of FTIR spectroscopy. Figure 5 (cf. spectrum 5E) shows a considerable shift in the position of the amide I band for API from 1634 to 1648 cm^{-1}, which could be attributed to an increase in alpha-helical structures (Yang *et al.*, 2009). The development of this type of conformation in others proteins after electrospinning has been previously reported (Hirota *et al.*, 1997; Stephens, Fahnestock, Farmer, Kiick, & Rabolt, 2005). However, some residual HFIP remains in the fibres (see arrows), fact that severely limits the applications of these structures in the medical, pharmaceutical, and food industries due to the intrinsic toxicity of this solvent. Therefore, alternative non-toxic solvents are desirable to obtain electrospun biopolymer structures (Ki *et al.*, 2005; Li, Cooper, Mauck, & Tuan, 2006).

INSERT FIGURE 5 ABOUT HERE

On the other hand, formic acid has been noted as a good organic solvent for various polypeptide-based polymers (Buchko *et al.,* 1999; Ki *et al.,* 2005; Um, Kweon, & Kwang,

2003; Wongsasulak *et al.*, 2007; Wongsasulak *et al.*, 2010), and moreover, it is a permitted food additive (Guidance for industry Q3C, 2003). Therefore, the suitability of formic acid for electrospinning of API was also studied. Three different amaranth protein concentrations (8, 10 and 20 %w/w) were evaluated, but the solution containing 20 wt.-% API was very viscous and gelled after some time, preventing the ejection of the polymer jet from the tip of the syringe. Capsule morphologies were obtained from the other two solutions (8 and 10 wt.-% API) as shown in Figure 6.

INSERT FIGURE 6 ABOUT HERE

Formic acid was a better solvent than acid acetic for API, but as shown in Figure 6, a fibrillar morphology was not attained with this solvent either. The differences in spinnability and morphology of the obtained structures can be, at least partially explained by the solution properties. Table 2 compiles the conductivity, surface tension and viscosity of the various API solutions in HFIP and formic acid. Comparing the formic and acetic acid solutions (compare Tables 1 and 2), the former shows increased viscosity and lower surface tension. This increase in the viscosity of proteins in formic acid has been previously reported (Van der Leeden *et al.*, 2003) and was attributed to unfolding and swelling of the globular polypeptide structure. The previous authors estimated from intrinsic viscosity measurements of β-lactoglobulin in formic acid that the volume of the polymer was approximately six times greater than that in water. The conformational change was further confirmed by circular dichroism spectroscopy which suggested a substantial increase in the percentage of random coil structures (Van der Leeden *et al.*, 2003). However, only small conformational changes were observed in the electrosprayed API structures obtained from

the formic acid solution (cf. spectrum C in Figure 5), since just a slight amide I band shift (from 1634 to 1638 cm^{-1}) was observed. According to other studies with amaranth protein isolates, disulfide bonds are involved in their structural stability (Avanza & Añon, 2007; Castellani, Martínez, & Añón, 1999). Therefore, intramolecular disulfide bridges add rigidity and stability to the protein structure, which could prevent the formation of continuous fibres. Moreover, as in the materials obtained from the HFIP solution, some residual solvent was also present in the API structures (see arrows indicating characteristic bands from formic acid).

Regarding the surface tension of the API solution in formic acid, it was considerably lower than that of the protein in acetic acid, fact which could have also favoured structure formation through electrospinning, although this surface tension was not low enough for fibre formation (Gupta *et al.,* 2005).

Table 2 shows that increasing protein concentration in both solvent solutions leads to a significant increase in both the viscosity and the conductivity of the solutions (the surface tension is mainly dependent on the type of solvent). Moreover, from Table 2 it can also be inferred that too high conductivity values are detrimental for fibre formation. It is known that increased conductivity results in a greater bending instability (Ramakrishna et al., 2005), which combined with relatively high surface tension values, only led to capsule or bead formation.

From Table 2 it can also be observed that significantly higher surface tension values were obtained for the formic acid solutions in comparison with those obtained with HFIP.

3.4 Effect of surfactants and mercaptoethanol addition on the morphology of electrospun API structures

In order to improve the spinnability of API in the formic acid solutions, different surfactants were evaluated. It is well-known that a high surface tension of the polymer solution may favour bead formation, whereas electrostatic forces due to charges within the jet have the tendency to elongate and maintain the jet to produce fibres (Ramakrishna *et al.*, 2005). The high surface tension of API solutions in formic acid might counteract the electrical forces, thus preventing the successful ejection of a steady polymer jet from the tip of the syringe. In order to reduce the surface tension of the formic acid solution, a food grade nonionic surfactant, Tween 80, an amphoteric surfactant, L-α-phosphatidylcholine and an anionic surfactant, Sodium stearoyl lactate (negative charge) were added to the biopolymer solutions. However, L-α-phosphatidylcholine and sodium stearoyl lactate (SSL) were not solubilized in the API-containing formic acid solution. This could be attributed to the interactions between the negative charges of the surfactants with the positive charges of the protein, generating insoluble polymer-surfactant complexes that rapidly phase separated from the solution (Kriegel, Kit, McClements, & Weiss, 2009).

On the other hand, addition of Tween 80 significantly improved the morphology of the electrospun structures (cf. Figure 7), which appears to be related with the decrease in the conductivity of the solutions (compare results of Table 2 and Table 3). The improved spinnability of polymeric solution by addition of this surfactant has been previously reported by others researchers (Kriegel*et al.,* 2009). From Table 3 it can be observed that the viscosity of the solutions was not significantly altered upon addition of Tween 80, and what it is even more surprising the surface tension was slightly increased (fact that could help explaining the smaller size of the capsules obtained).

INSERT TABLE 3 ABOUT HERE

On the other hand, conductivity was significantly reduced, which seems to be a key factor for explaining the improved morphology of the electrosprayed materials. The reduction in conductivity could be explained by the binding of surfactant monomers to the backbone of API, thereby reducing its polyelectrolytic character (Kriegel *et al.*, 2009). From Figure 7, it seems that addition of 20 wt.-% of Tween 80 resulted in improved morphologies in comparison with the structures obtained from the protein solution containing just 10 wt.-%. The lower surface tension and conductivity of the former solution could, at least partially explain this result (cf. Table 3).

INSERT FIGURE 7 ABOUT HERE

The other strategy attempted to improve the spinnability of the protein solution in formic acid was addition of 2-mercaptoethanol (2-ME), as this substance contributes to denaturation of proteins by reducing disulfide linkages. Figures 5C and 5D show the scanning electron microscopic images obtained using 2-ME and the reducing agent combined with Tween 80, respectively. From the images it seems that the combination of 2-ME with the surfactant provided considerably better results, although no fibres were obtained. Figure 8 shows the ATR-FTIR spectra of the structures with 20% of surfactant and with the combination of surfactant and reducing agent. Both the addition of 20% of Tween 80 and Tween 80 with 2-ME led to an increase in alpha helical structures as inferred by the amide I shift from 1634 to 1650 cm^{-1} and 1647 cm^{-1}, respectively (Yang *et al.*, 2009) and, moreover, taking into account that band width is a measure of conformational freedom (Barth, 2007), the structures developed using Tween 80 and with the combination of the

surfactant and the reducing agent displayed narrower bands indicating the formation of more rigid structures. Comparing the solution properties using HFIP and formic acid with the additives (Tables 2 and 3) it seems that apart from denaturing the protein structure, lower conductivity and surface tension values are needed for fibre development.

4. Conclusions.

Amaranth protein isolate (API)-based ultrathin structures have been developed for the first time using electrospinning. The morphology of the resulting structures was mainly affected by the appropriate choice of solvent and the protein concentration. Fibre morphologies were only obtained using HFIP as the API solvent, while capsule morphologies were developed from formic acid solutions. Addition of Tween 80 and a combination of this surfactant with the reducing agent 2-mercaptoethanol resulted in improved morphology of the encapsulates and to enhanced spinnability of the API-containing formic acid solutions. This study has also demonstrated that the ability to generate encapsulation structures from API depends, not only on the protein conformation, but also on the solution properties (conductivity, surface tension and viscosity). The API structures generated from formic acid solutions could find applications as new food ingredients or as encapsulation structures for food ingredients.

5. Acknowledgements.

The authors acknowledge Dr. Benito Manrique de Lara y Soria for providing the amaranth protein concentrate used in this study. A. Lopez-Rubio is recipient of a Ramon y Cajal contract from the Spanish Ministry of Science and Innovation. The authors thank the

504 Spanish MICINN projects MAT2009-14533-C02-01, FUN-C-FOOD (CSD2007-00063),
505 and Mexican project FOMIX-QRO-2011-C02-175350 for financial support and Mexican
506 National Council for Science and Technology (CONACYT) for a graduate fellowship, to
507 author Marysol Aceituno-Medina.
508

6. References.

Abugoch, E. L., Martínez, N. E., &Añón, M. C. (2010). Influence of pH on structure and function of amaranth (*Amaranthus hypochondriacus*) protein isolates. *Cereal Chemistry,87*, 448-453.

Avanza, M. V., & Añón M. C. (2007). Effect of thermal treatment on the proteins of amaranth isolates. *Journal of the Science of Food and Agriculture, 87*, 616-623.

Barth, A. (2007). Infrared spectroscopy of proteins. *Biochimica et Biophysica Acta (BBA)–Bioenergetics, 1767*, 1073-1101.

Buchko, C. J., Chen, L. C., Shen, Y., & Martin, D. C. (1999). Processing and microstructural characterization of porous biocompatible protein polymer thin films. *Polymer, 40*, 7397–7407.

Castellani, O. F., Martínez, E. N., & Añón, M. C. (1999). Role of disulfide bonds upon the structural stability of an amaranth globulin. *Journal of Agricultural and Food Chemistry, 47*, 3001-3008.

Chakraborty, S., Liao, I-C., Adler, A., & Leong K. W. (2009). Electrohydrodynamics: A facile technique to fabricate drug delivery systems. *Advanced Drug Delivery Reviews, 61*, 1043-1054.

Colla, E., Sobral, P. J. A., & Menegalli, F.C. (2006). *Amaranthus cruentus* flour edible films - Influence of stearic acid addition, plasticizer concentration and the emulsion stirring speed on water vapor permeability and mechanical properties. *Journal and Agricultural and Food Chemistry, 36*, 249-254.

Dror, Y., Ziv, T., Makarov, V., Wolf, H., Admon, A., & Zussman, E. (2008). Nanofibres made of globular proteins. *Biomacromolecules,9*, 2749–2754.

Drzewiecki, J., Delgado-Licon, E., Haruenkit, R., Pawelzik, E., Martin-Belloso, O., Park, Y-S., Jung, S.-T., Trakhtenberg, S., & Gorinstein, S. (2003). Identification and differences of total proteins and their soluble fractions in some pseudocereals based on electrophoretic patterns. *Journal and Agricultural and Food Chemistry, 51*, 7798-7804.

Elizondo, N. J., Sobral, P. J. A., & Menegalli, F. C. (2009). Development of films based on blends of *Amarantus cruentus* flour and poly(vinyl alcohol). *Carbohydrate Polymers, 75*, 592-598.

Gorinstein, S., Pawelzik, E., Delgado-Licon, E., Haruenkit, R., Weisz, M., & Trakhtenberg, S. (2002). Characterisation of pseudocereal and cereal proteins by protein and amino acid analyses. *Journal of the Science of Food and Agriculture, 82*, 886-891.

Guidance for industry Q3C — Tables and List. 2003. Food and Drug administration. Office of Communication, Training, and Manufacturers Assistance (HFM-40). http://www.fda.gov/cber/guidelines.htm.

Gupta, P., Elkins, C., Long, T., & Wilkes, G. (2005). Electrospinning of linear homopolymers of poly(methyl methacrylate): exploring relationship between fibre formation, viscosity, molecular weight and concentration in a good solvent. *Polymer, 46*, 4799-4810.

Heunis, T. D. J., Botes, M., & Dicks, L. M. T. (2010). Encapsulation of *Lactobacillus plantarum* 423 and its bacteriocin in nanofibres. *Probiotics and Antimicrobial Proteins, 2*, 46-51.

Hirota, N., Mizuno, K., & Goto, Y. (1997). Cooperative α-helix formation of β-lactoglobulin and melittin induced by hexafluoroisopropanol. *Protein Science, 6*, 416-421.

554 Ki, C. S., Baek, D. H., Gang, K. D., Lee, K. H., Um, I. C., & Park, Y. H. (2005).
555 Characterization of gelatin nanofibre prepared from gelatin–formic acid solution. *Polymer*,
556 *46*, 5094–5102.
557 Konishi, Y., Fumita, Y., Ikeda, K., Okuno, K. & Fuwa, H. (1985). Isolation and
558 characterization of globulin from seeds of *Amaranthus hypochodriacus*. *Biological*
559 *Chemistry, 45*, 1453-1459.
560 Konishi, Y., Horikawa, K., Oku, J., Azumaya, J., & Nakatani, N. (1991). Extraction of two
561 albumin fractions from amaranth grains: comparison of some physico-chemical properties
562 and the putative localization in the grains. *Agricultural and Biological Chemistry, 55*, 2745-
563 2750.
564 Kriegel, C., Kit, K. M., McClements, D. J., & Weiss, J. (2009). Electrospinning of
565 chitosan–poly(ethylene oxide) blend nanofibres in the presence of micellar surfactant
566 solutions. *Polymer, 50*, 189–200.
567 Li, D., McCann, J. T., & Xia, Y. N. (2005). Use of electrospinning to directly fabricate
568 hollow nanofibres with functionalized inner and outer surfaces. *Small, 1*, 83–86.
569 Li, W. J., Cooper, J. A., Mauck, R. L., & Tuan, R. S. (2006). Fabrication and
570 characterization of six electrospun poly(alpha-hydroxy ester)-based fibrous scaffolds for
571 tissue engineering applications. *Acta Biomaterialia, 2*, 377– 385.
572 Li, Y., Lim, L. T., & Kakuda, Y. (2009). Electrospun zein fibres as carriers to stabilize (−)-
573 Epigallocatechin Gallate. *Journal of Food Science, 74*, 233-240.
574 Lopez-Rubio, A. & Lagaron, J. M. (2012). Whey protein capsules obtained through
575 electrospraying for the encapsulation of bioactives. *Innovative Food Science and Emerging*
576 *Technologies, 13*, 200-206.

577 Lopez-Rubio, A., Sanchez, E., Sanz, Y., & Lagaron, J. M. (2009). Encapsulation of living
578 bifidobacteria in ultrathin PVOH electrospun fibres. *Biomacromolecules, 10*, 2823-2829.
579 Lopez-Rubio, A., Sanchez, E., Wilkanowicz, S., Sanz, Y., & Lagaron, J. M. (2012).
580 Electrospinning as a useful technique for the encapsulation of living Bifidobacteria in food
581 hydrocolloids. *Food Hydrocolloids, 28*, 159-167.
582 Marcone, M. F. (1999). Evidence confirming the existence of a 7S globulin-like storage
583 protein in *Amaranthus hypochondriacus* seed. *Food Chemistry, 65*, 533-542.
584 Martínez, E. N., & Añon, M. C. (1996). Composition and structural characterization of
585 amaranth protein isolates. An electrophoretic and calorimetric study. *Journal of*
586 *Agricultural and Food Chemistry*, *44*, 2523-2530.
587 Matthews, J. A., Wnek, G. E., Simpson, D. G., & Bowling, G. L. (2002). Electrospinning
588 of collagen nanofibres. *Biomacromolecules, 3*, 232-238.
589 P201131705 Patent Application (2011). Micro-, submicro y nanoestructuras basadas en
590 proteína de amaranto. Inventors: A. López-Rubio, J.M. Lagaron, M. Aceituno-Medina & S.
591 Mendoza. Holder entity: CSIC & University of Querétaro.
592 Quiroga, A. V., Martínez, E. N., & Añón, M. C.(2007). Amaranth globulin polypeptide
593 heterogeneity. *Protein Journal, 26*, 327-333.
594 Rajendran, S., & Prakash, V. (1988). Association-dissociation and denaturation-
595 renaturation of high-molecular-weight protein: carmin from safflower seed (*Carthamus*
596 *tinctorius* L.) in alkaline solution. *Journal of Protein Chemistry, 7*, 689-712.
597 Ramakrishna, S., Fujihara, K., Teo, W-E., Lim, T-C., & Ma, Z. (2005). *An introduction to*
598 *electrospinning and nanofibres*. (pp. 69-102). World Scientific Publishing.
599 Reneker, D. H., & Chun, I. (1996). Nanometre diameter fibres of polymer, produced by
600 electrospinning. *Nanotechnology, 7*, 216-223.

Salcedo-Chávez, B. Osuna-Castro, J. A., Guevara-Lara, F., Domínguez-Domínguez, J., & Paredes-López, O. (2002). Optimization of the isoelectric precipitation method to obtain protein isolates from amaranth (*Amaranthus cruentus*) seeds. *Journal of Agricultural and Food Chemistry, 50*, 6515-6520.

Schiffman, J. D. & Schauer, C. L. (2008). A review: Electrospinning of biopolymer nanofibers and their applications. *Polymer Reviews, 48*, 317-352.

Schnetzler, K. A., & Breen, W. M. (1994). Food Uses and Amaranth Product Research: A Comprehensive Review. In O. Paredes-López (Ed.), *Amaranth: Biology, Chemistry, and Technology* (pp. 155–184). Boca Raton: CRC Press.

Scilingo, A., Molina, S., Martínez, N., & Añón. M. C. A. (2002). Amaranth protein isolates modified by hydrolytic and thermal treatments. Relationship between structure and solubility. *Food Research International, 35*, 855-862.

Silva-Sánchez, C., Barba de la Rosa, A. P., León-Galván, M. F., De Lumen B. O., De León-Rodríguez, A., & González de Mejía, E. (2008). Bioactive peptides in amaranth (*Amaranthus hypochondriacus*) seed. *Journal of Agricultural and Food Chemistry, 56*, 1233–1240.

Stephens, J. S., Fahnestock, S., Farmer, R., Kiick, K., & Rabolt, J. (2005). Effects of electrospinning and solution casting protocols on the secondary structure of a genetically engineered dragline spider silk analogue investigated via Fourier transform Raman spectroscopy. *Biomacromolecules, 6*, 1405-1413.

Tapia-Blácido, D., Mauri, A., Menegalli, F. C., & Sobral, P. J. A. (2005). Development and characterization of edible films based on amaranth flour (*Amarantus caudatus*). *Journal of Food Engineering, 67*, 215-223.

624 Teutonico, R. A., & Knorr, D. (1985). Non-destructive method for oxalate determination of
625 cultured *Amaranthus tricolor* cells. *Journal of Agricultural and Food Chemistry, 33*, 60-62.
626 Torres-Giner, S., Gimenez, E., & Lagaron, J. M. (2008). Characterization of the
627 morphology and thermal properties of zein prolamine nanostructures obtained by
628 electrospinning. *Food Hydrocolloids, 22*, 601–614.
629 Torres-Giner, S., Martinez-Abad, A., Ocio, M. J., & Lagaron, J. M. (2010). Stabilization of
630 a nutraceutical omega-3 fatty acid by encapsulation in ultrathin electrosprayed zein
631 prolamine. *Journal of Food Science, 75*, N69-N79.
632 Um, C., Kweon, H., & Kwang, L. (2003). The role of formic acid in solution stability and
633 crystallization of silk potein polymer. *International Journal of biological Macromolecules,*
634 *33*, 203-213.
635 Van der Leeden, M. C., Rutten, A. A. C. M., & Frens, G. (2000). How to develop globular
636 proteins into adhesives. *Journal of Biotechnology, 79*, 211–221.
637 Ventureira, J. L., Bolontrade, A. J., Speroni, F., David-Briand, E., Scilingo, A. A., Ropers,
638 M.-H., Boury, F., Añon, M. C., & Anton, M. (2012). Interfacial and emulsifying properties
639 of amaranth (*Amarantus hypochondriacus*) protein isolates under different conditions of
640 pH. *LTW-Food Science and Technology, 45*, 1-7.
641 Woerdeman, D. L., Ye, P., Shenoy, S., Parnas, R. S., Wnek, G. E., & Trofimova, O. (2005).
642 Electrospun fibres from wheat protein: Investigation of the interplay between molecular
643 structure and the fluid dynamics of the electrospinning process. *Biomacromolecules, 6*,
644 707-712.
645 Wongsasulak, S., Kit , K. M., Mcclements, D.-J., Yoovidhya, T., & Weiss, J. (2007). The
646 effect of solutions properties of the morphology of ultrafine electrospun egg albumen-PEO
647 composite fibres. *Polymer, 48*, 448-457.

Wongsasulak, S., Patapeejumruswong, M., Weiss, J., Supaphol, P., & Yoovidhya, T. (2010). Electrospinning of food-grade nanofibres from cellulose acetate - egg albumen blends. *Journal of Food Engineering, 98,* 370-376.

Xu, X., Yang, Q., Wang, Y., Yun, H., Chen, X., & Jing, X. (2006). Biodegradable electrospun poly(L-lactide) fibres containing antibacterial silver nanoparticles. *European Polymer Journal, 42*, 2081–2087.

Yang, X., Dacheng, W., Zongliang, D., Ruixia, L., Xulong, C., & Xiaohui, L. (2009). Spectroscopy study on the interaction of quercetin with collagen. *Journal of Agricultural and Food Chemistry,57*, 3431–3435.

Figure captions

Figure 1. Electrophoretic profile of amaranth protein isolate (API): a) standards; b) SDS-PAGE with 2-ME; c) SDS-PAGE without 2-ME.

Figure 2. SEM (a, c, e, g) and optical microscope (b, d, f, h) images of API electrospun structures from acetic acid (50/50 %v/v) and sodium hydroxide (0.01M) solutions at different pH: pH 2 (a, b); pH 2 heating (c, d); pH 12 (e, f); pH 12 heating (g, h). Scale bar: 5 µm.

Figure 3. ATR-FTIR spectra of: (A) Acetic acid; (B) Amaranth protein isolate (API); (C) Electrosprayed API from acetic acid solution; (D) Same as (C) after drying at 60ºC during 30 minutes. Dotted line indicates the position of the band related to β-sheet structures. Arrows point out to characteristic bands arising from the presence of solvent in the structures. Spectra have been offset for clarity.

Figure 4. SEM images of electrospun amaranth fibers obtained from HFIP solutions at different protein concentrations: a) 5%; b) 8%; c) 10% w/w. Scale bar: 20 µm.

Figure 5. ATR-FTIR spectra of: (A) Amaranth protein isolate (API); (B) Formic acid; (C) Electrosprayed API from formic acid solution; (D) HFIP; (E) Electrospun API structures from HFIP solution. Dotted line indicates the position of the band related to β-sheet structures present in API. Arrows point out to characteristic bands arising from the presence of solvent in the structures. Spectra have been offset for clarity.

Figure 6. SEM images of electrospun amaranth structures obtained from formic acid solutions at different protein concentrations: a) 8%; b) 10%. Scale bar: 5 µm.

Figure 7. SEM images of amaranth structures obtained from formic acid solutions containing: a) 10% Tween80; b) 20% Tween80; c) 20% 2-mercapthoethanol; d) 15% Tween 80 + 20% 2-mercapthoethanol.

Figure 8. ATR-FTIR spectra of: (A) Amaranth protein isolate (API); (B) Tween80; (C) Electrosprayed API from formic acid solution containing 20% Tween80; (D) Electrosprayed API from formic acid solution containing 15% Tween80 + 20% 2-mercaptoethanol. Dotted line indicates the position of the band related to β-sheet structures present in API. Spectra have been offset for clarity.

Figure 1

Click here to download high resolution image

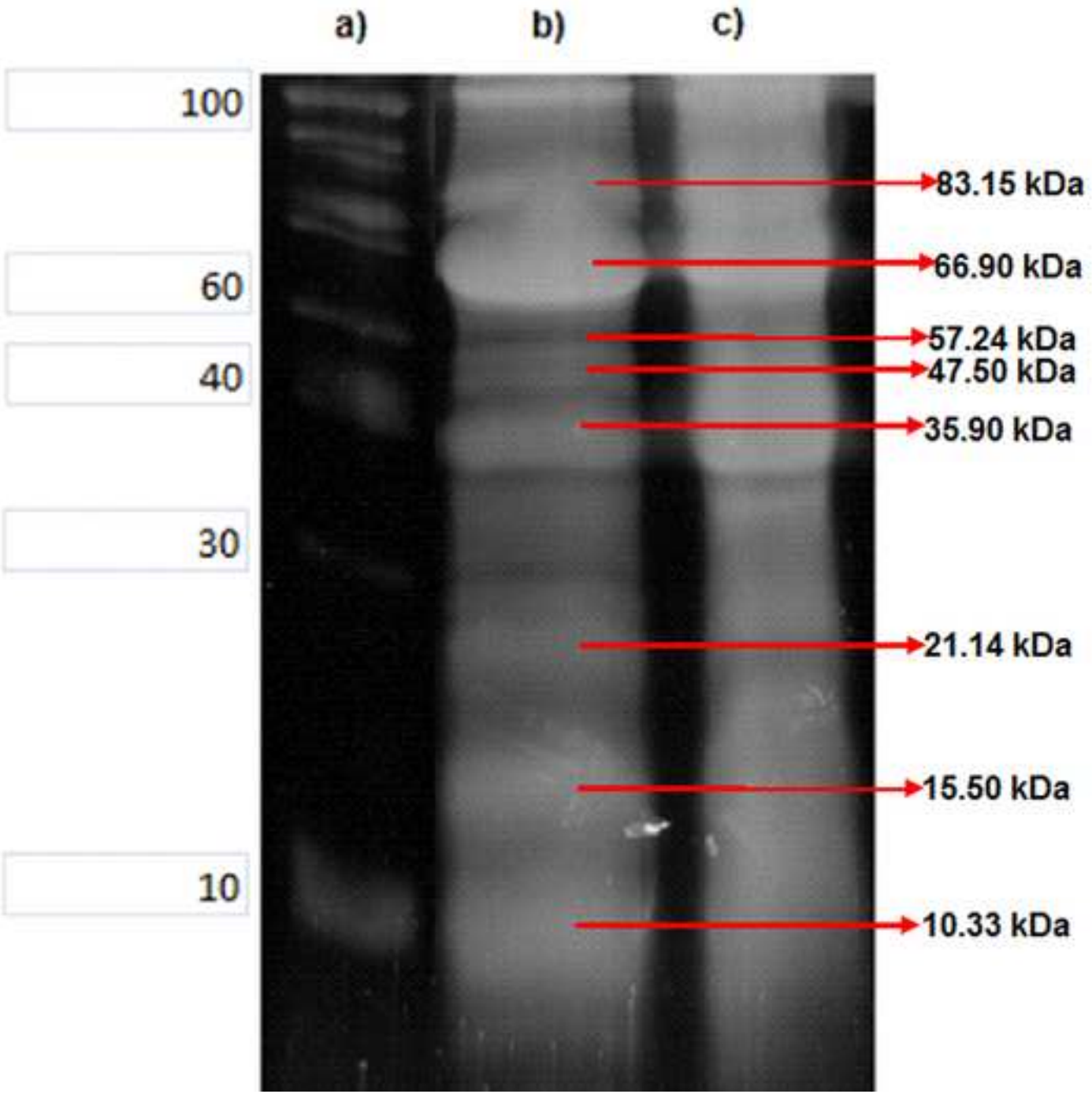

Figure 2

Click here to download high resolution image

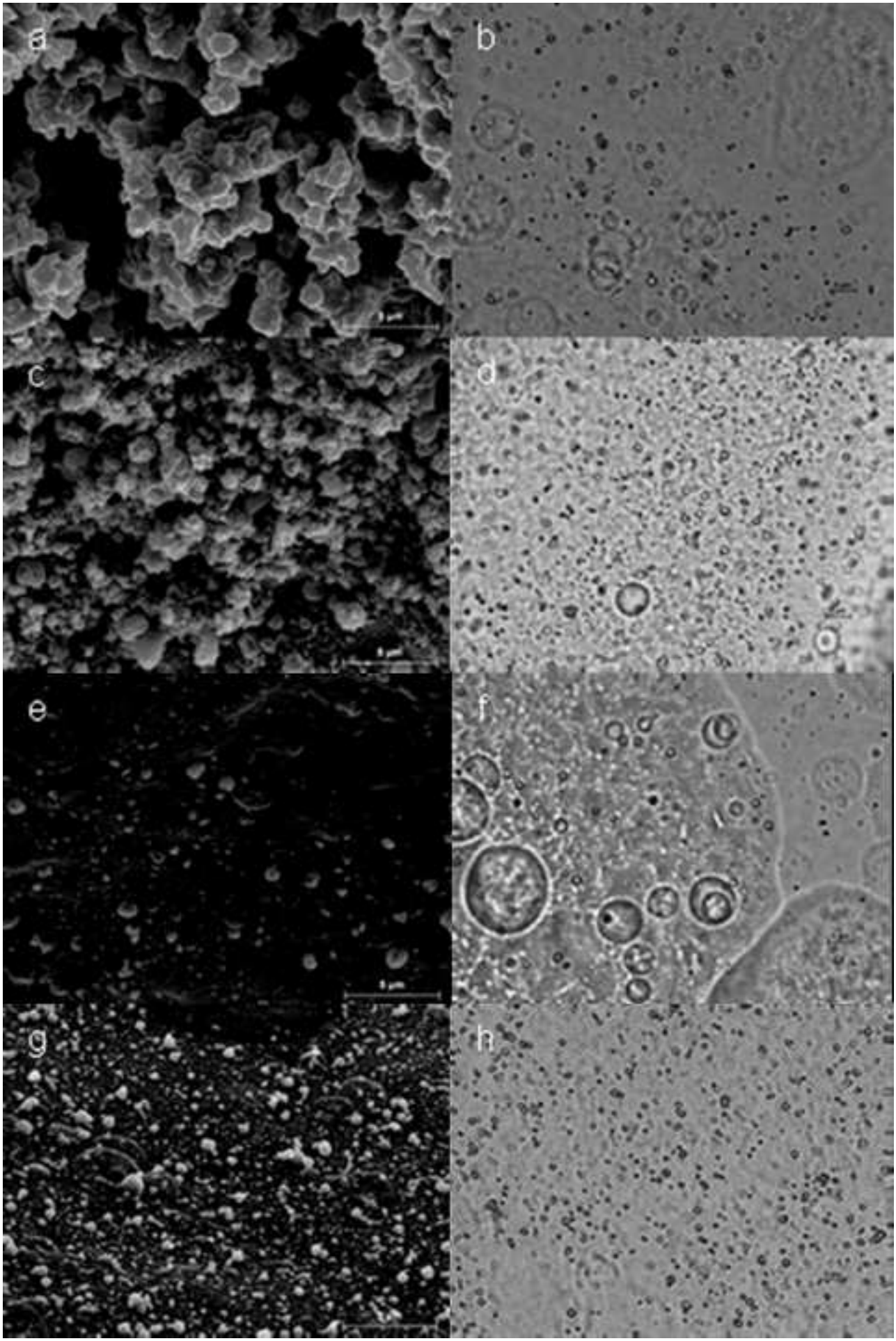

Figure 3

Click here to download high resolution image

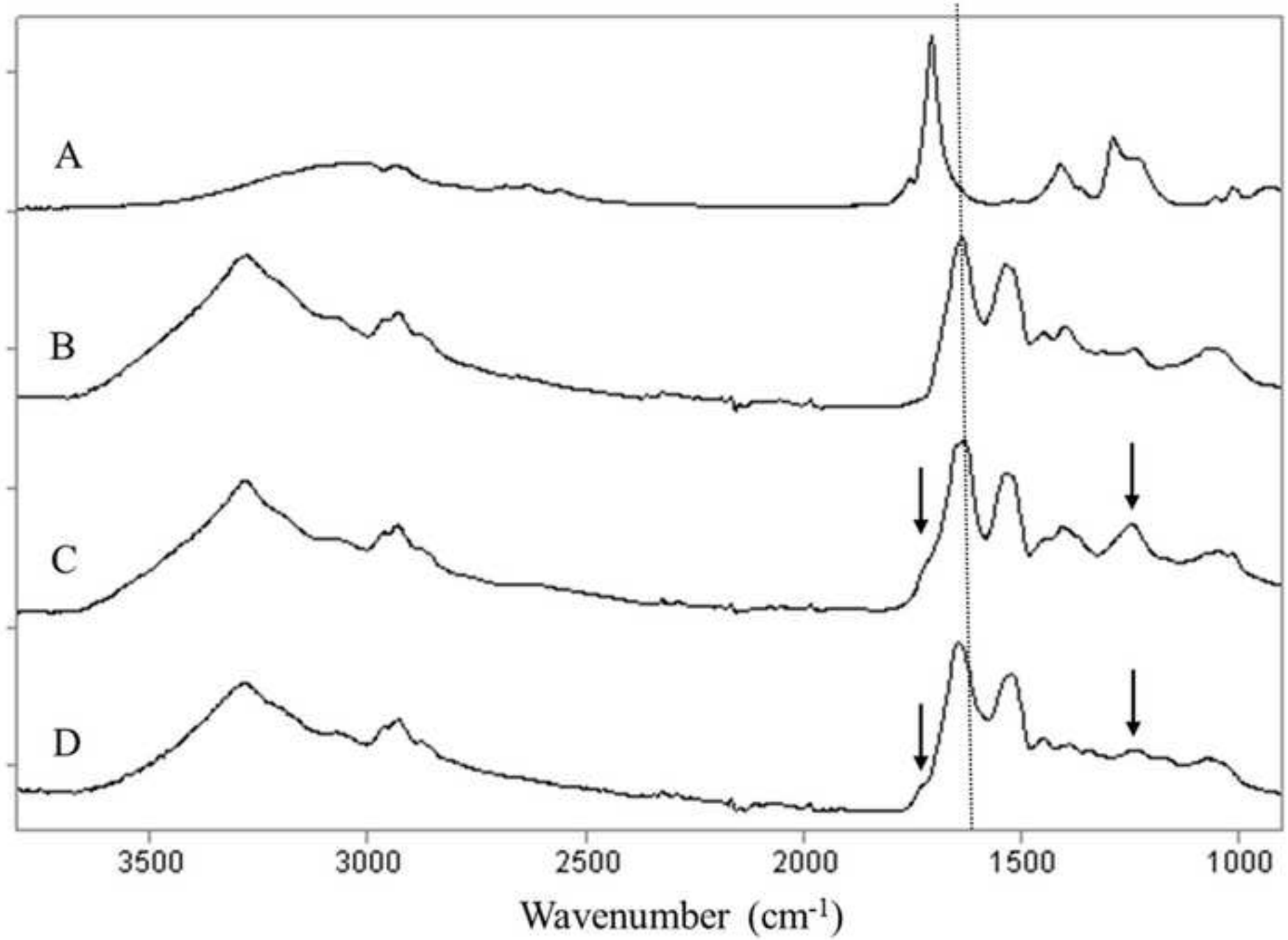

Figure 4A

Click here to download high resolution image

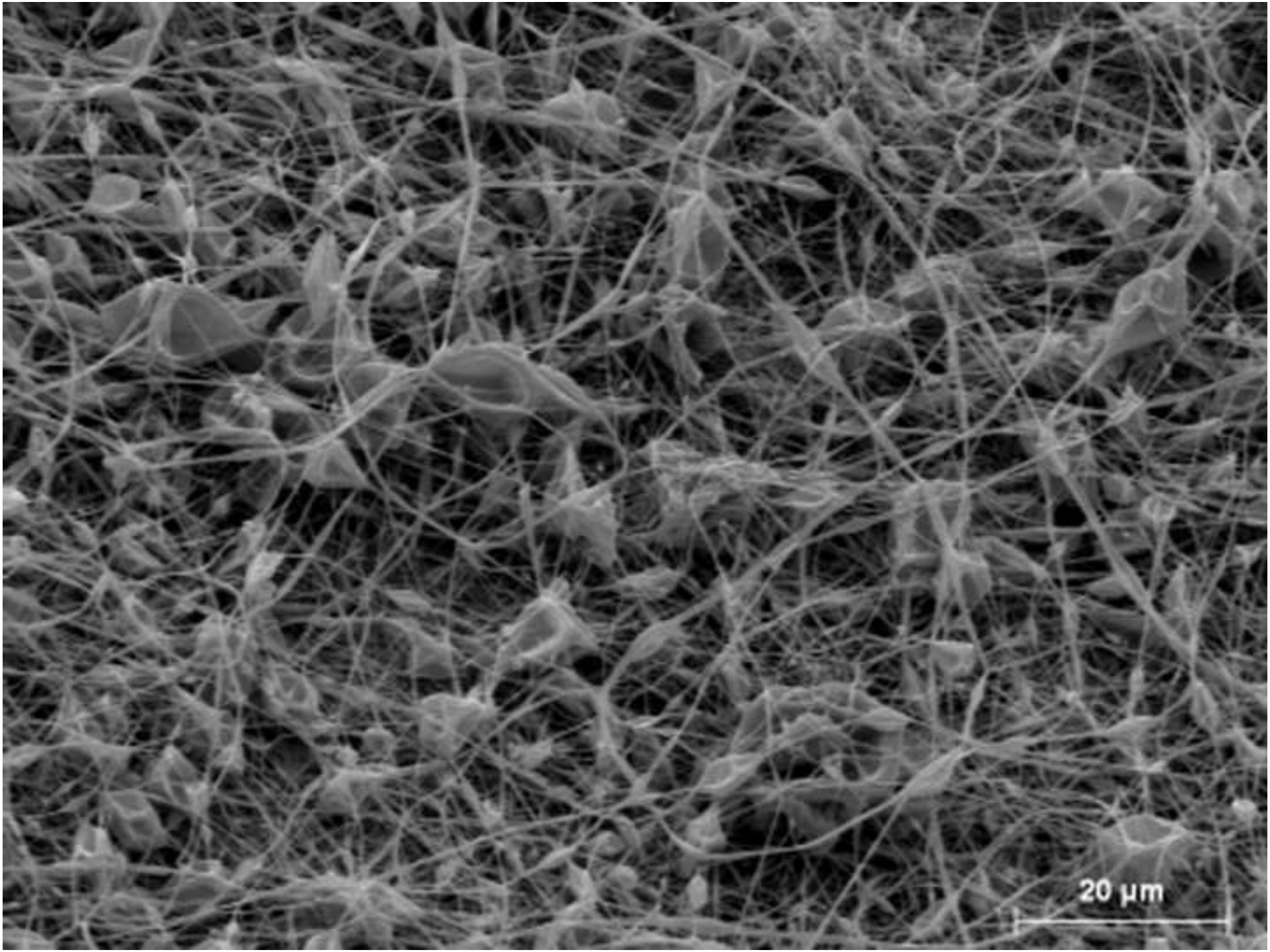

Figure 4B

Click here to download high resolution image

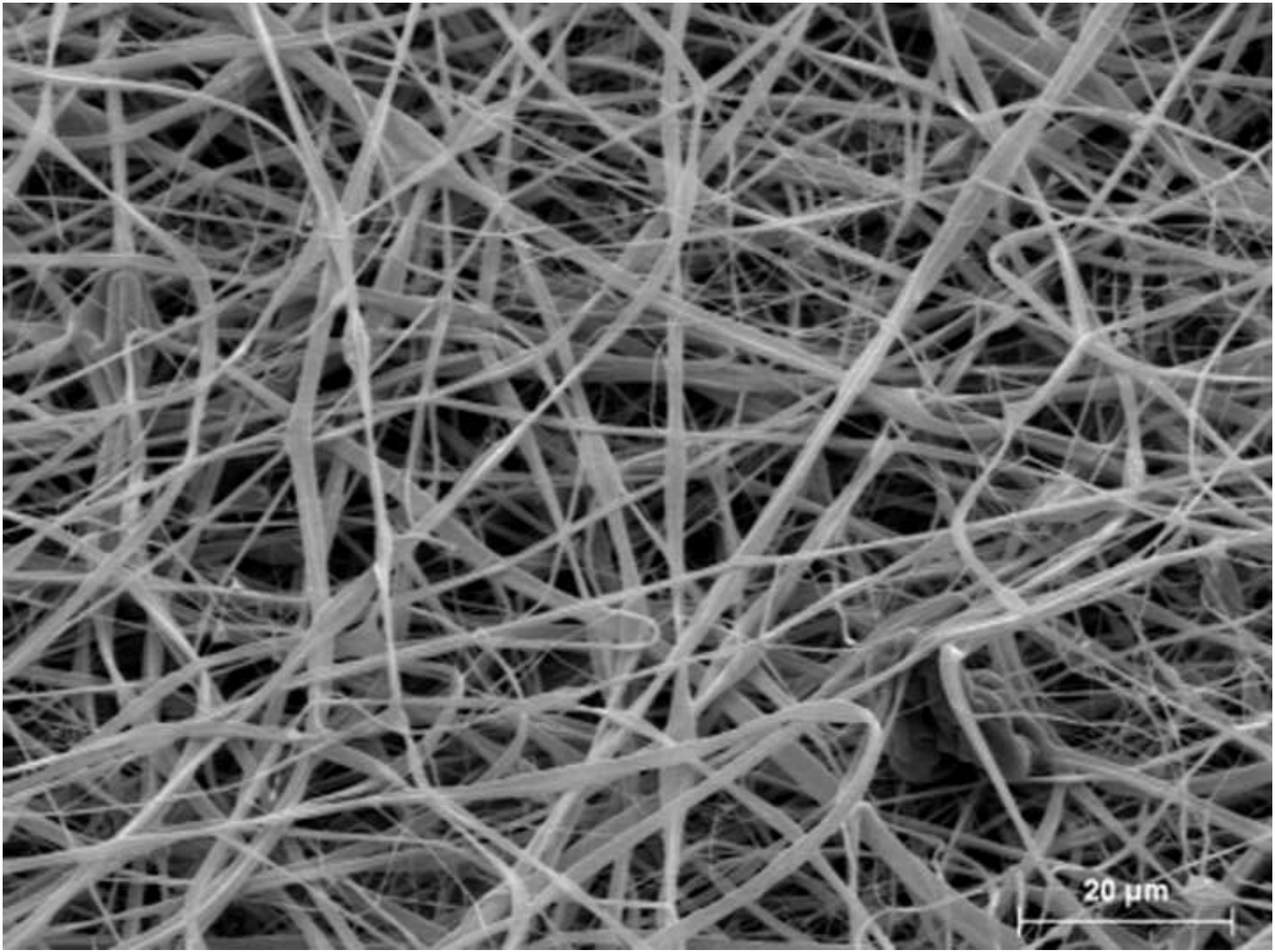

Figure 4C

Click here to download high resolution image

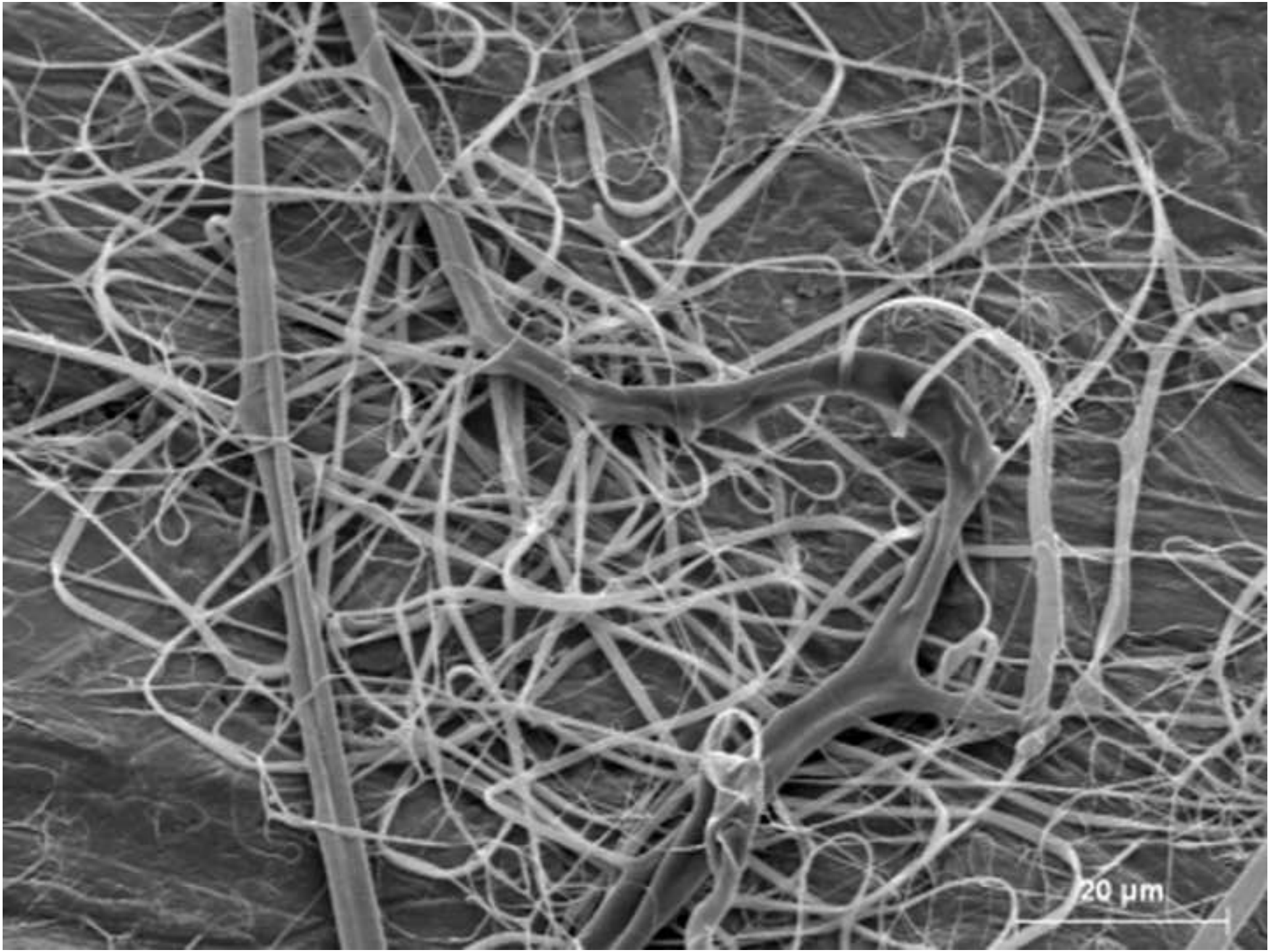

Figure 5

Click here to download high resolution image

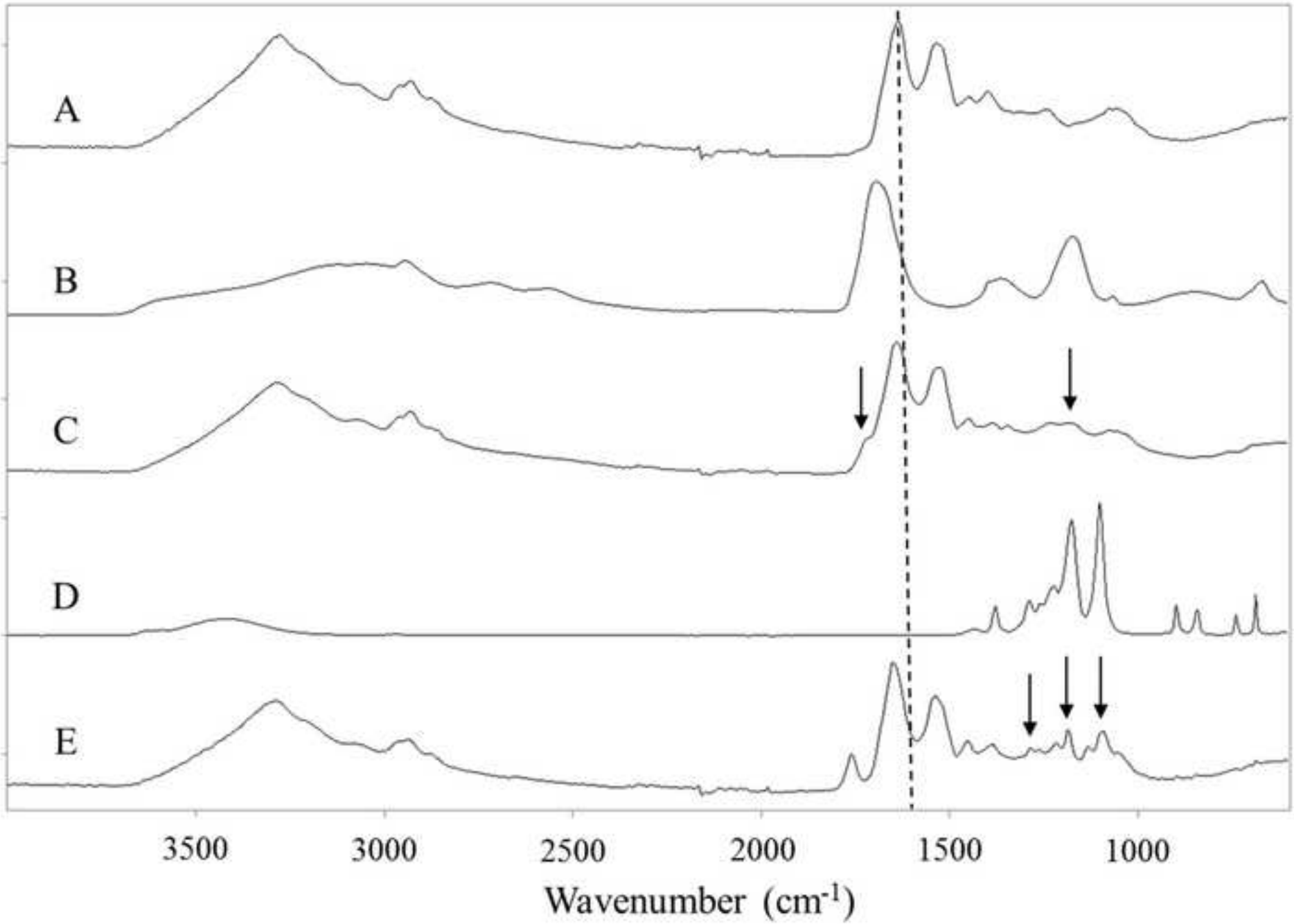

Figure 6A

Click here to download high resolution image

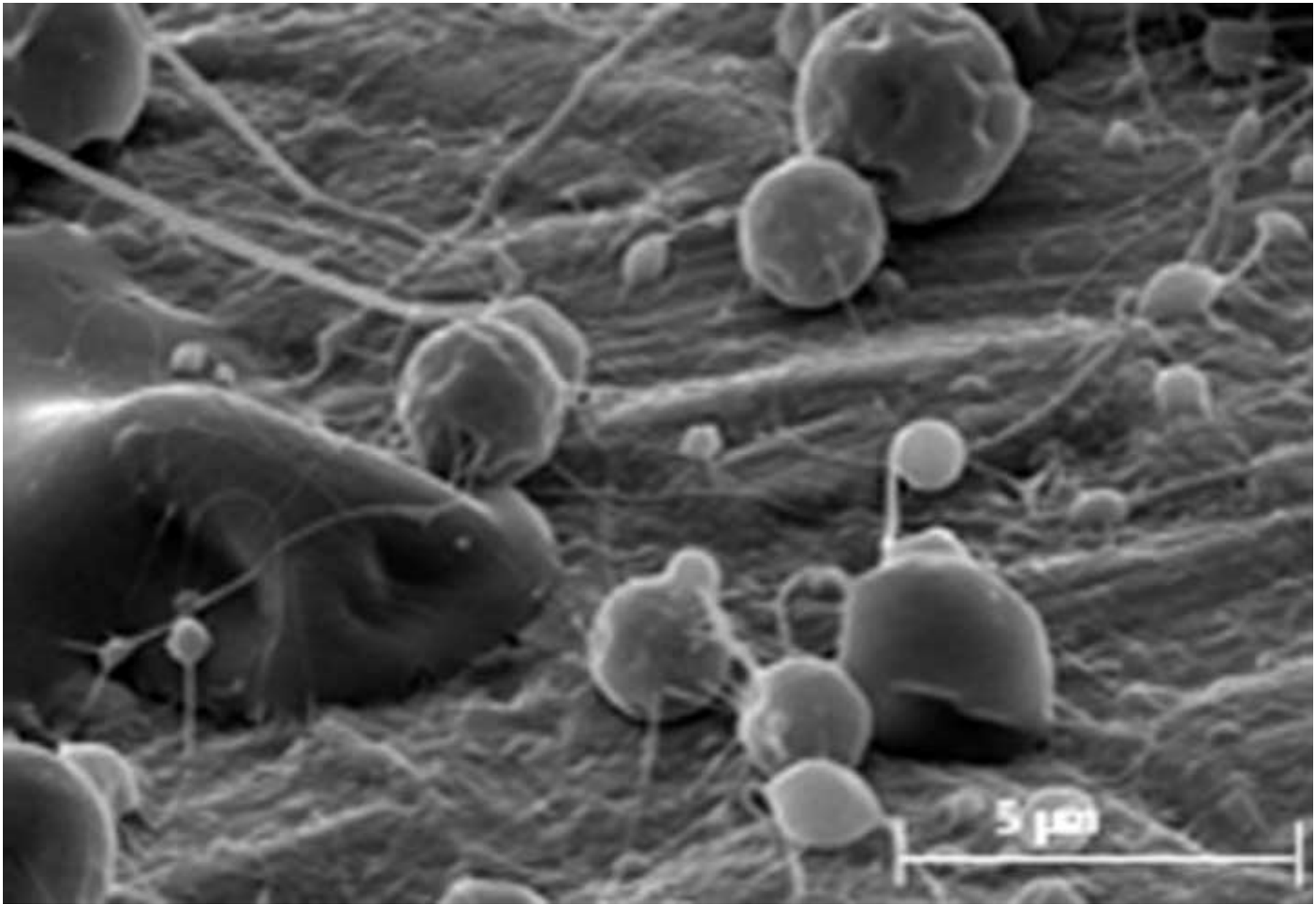

Figure 6B

Click here to download high resolution image

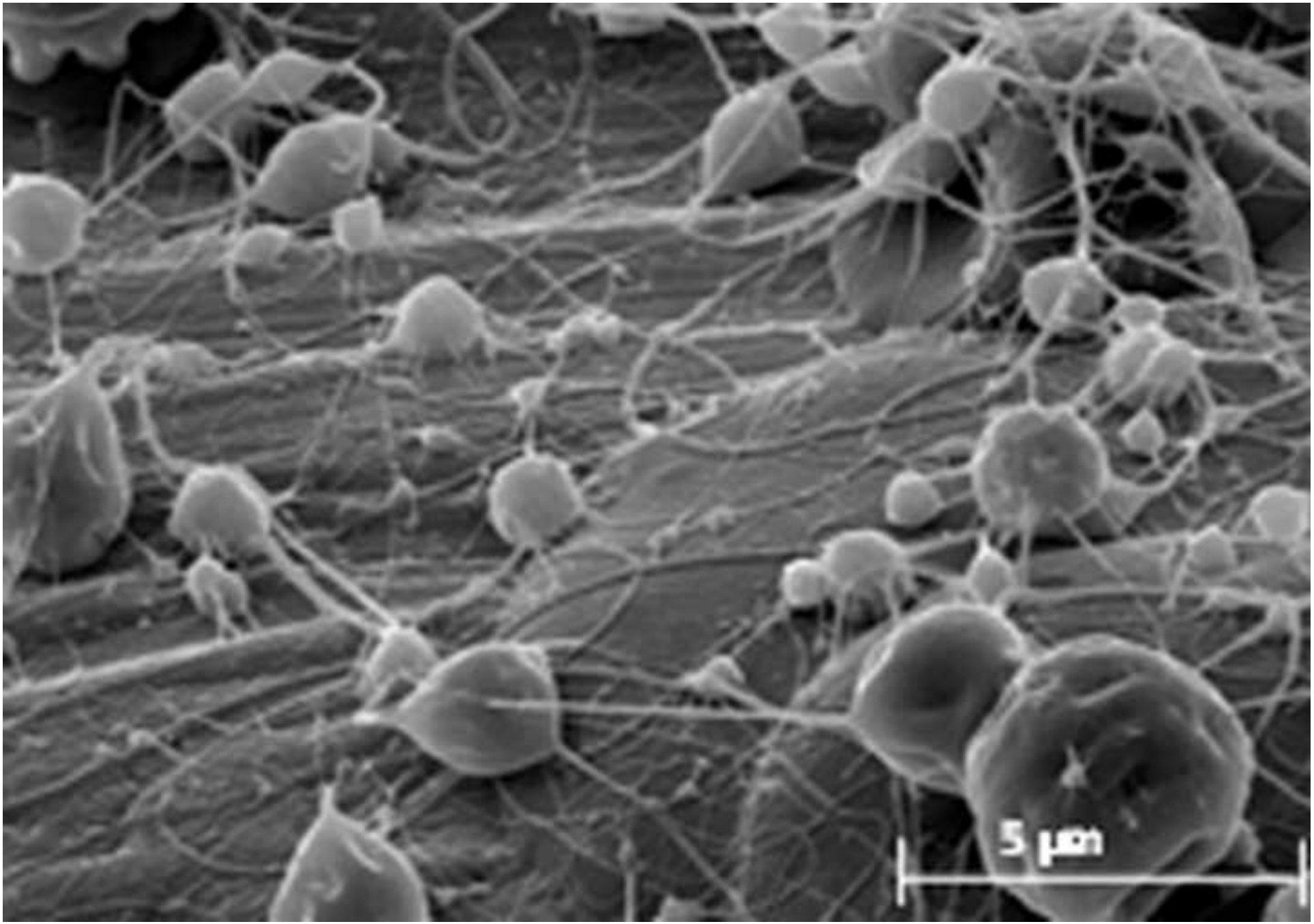

Figure 7A

Click here to download high resolution image

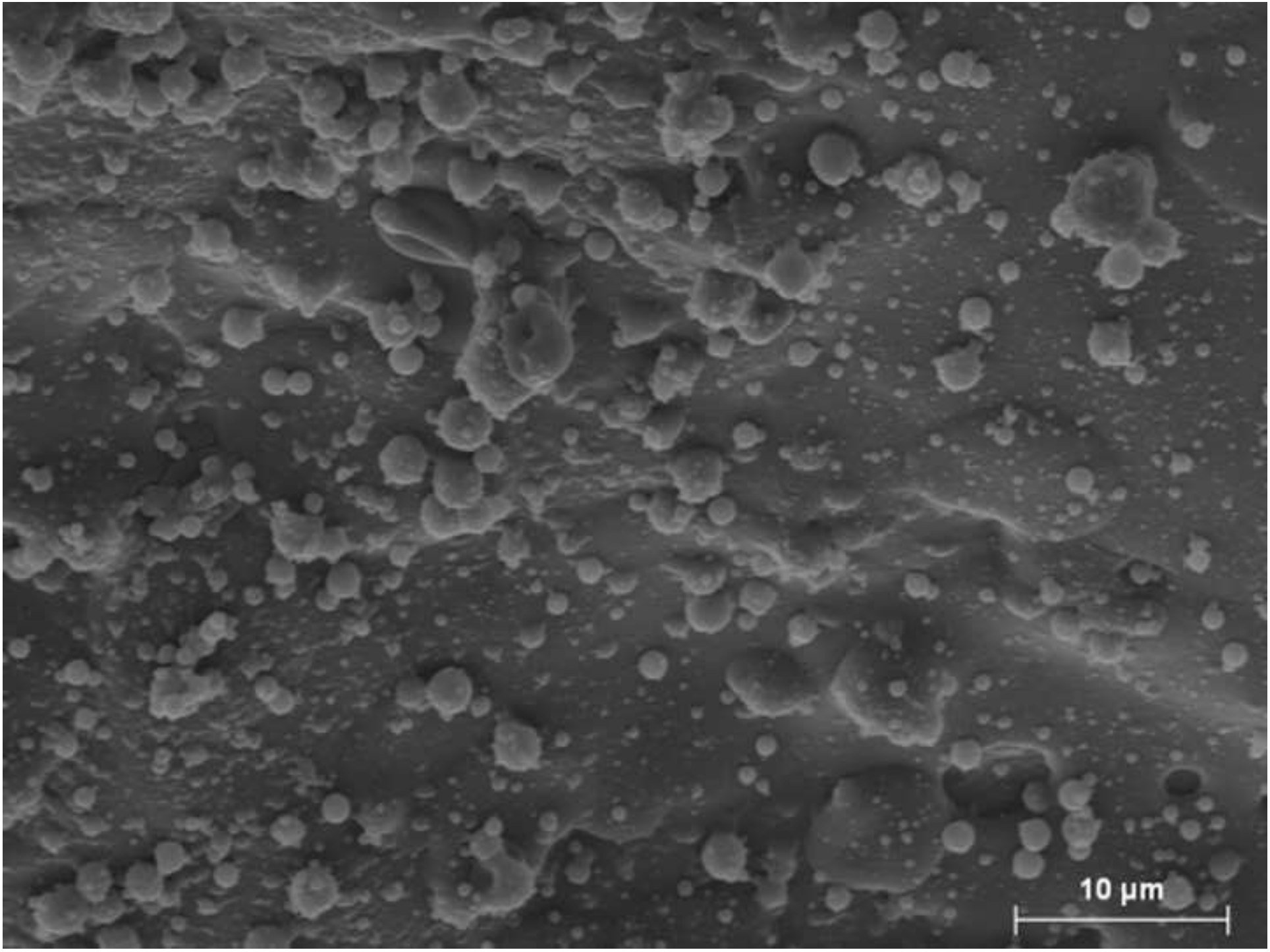

Figure 7B

Click here to download high resolution image

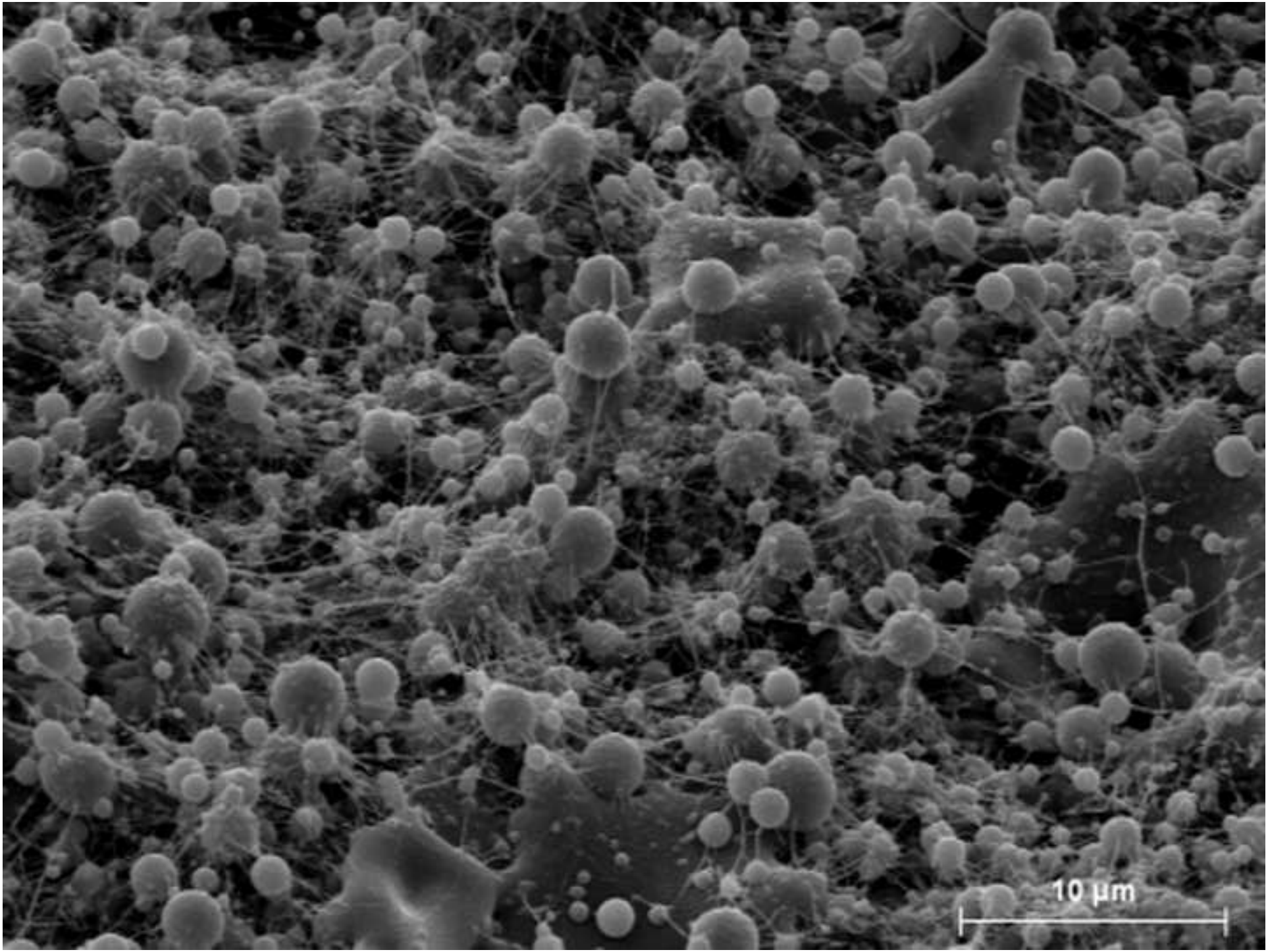

Figure 7C

Click here to download high resolution image

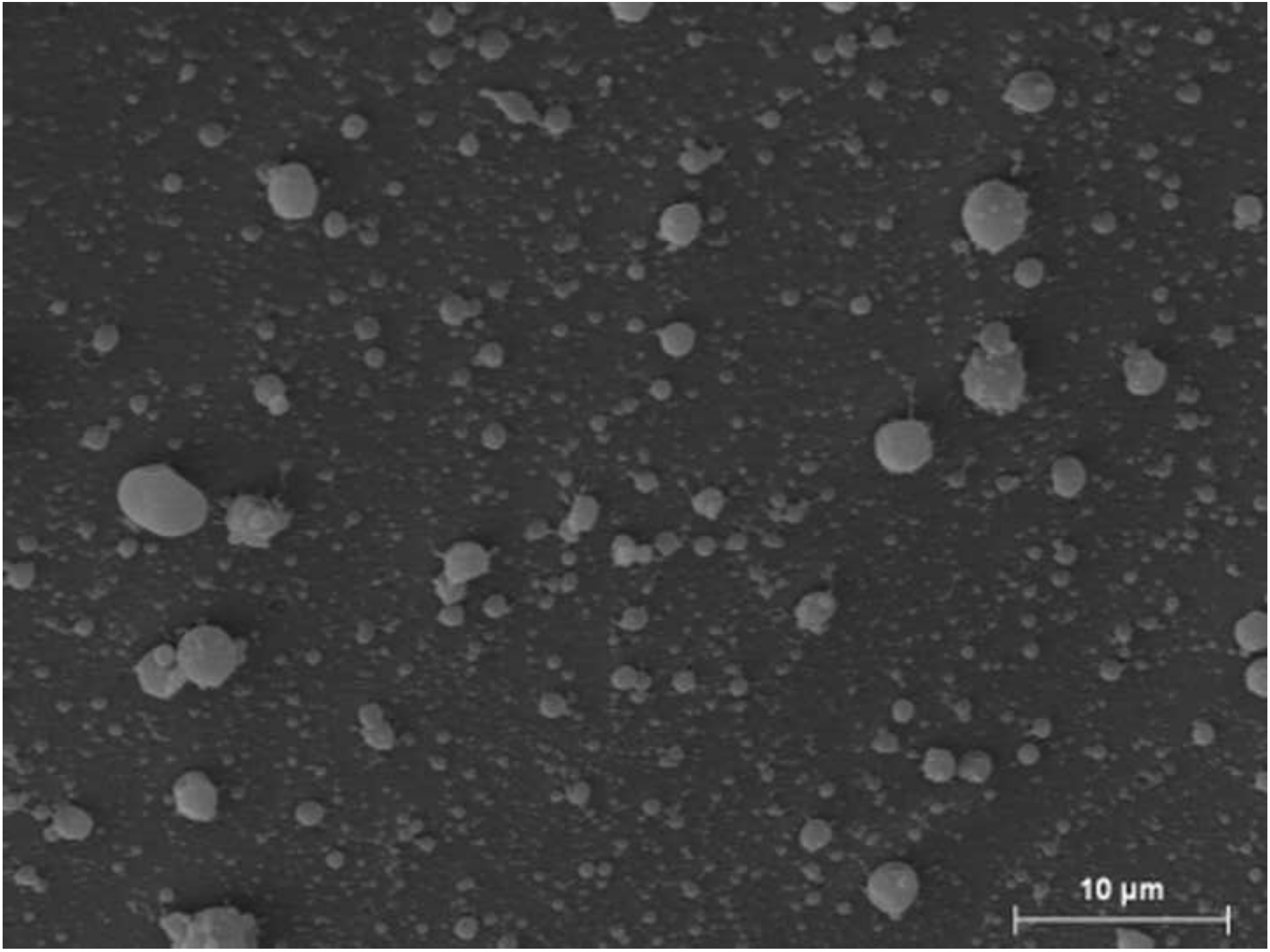

Figure 7D

Click here to download high resolution image

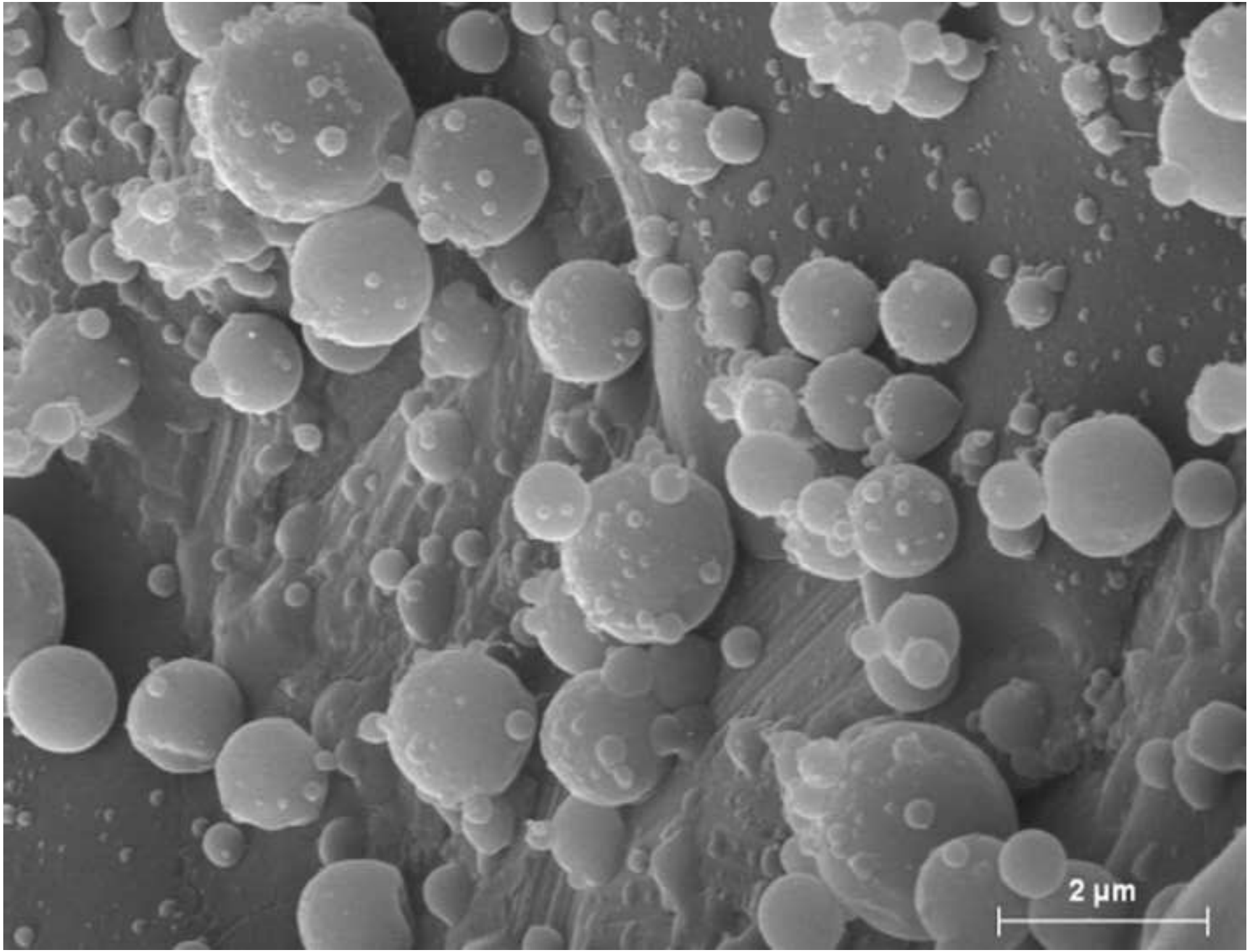

Figure 8

Click here to download high resolution image

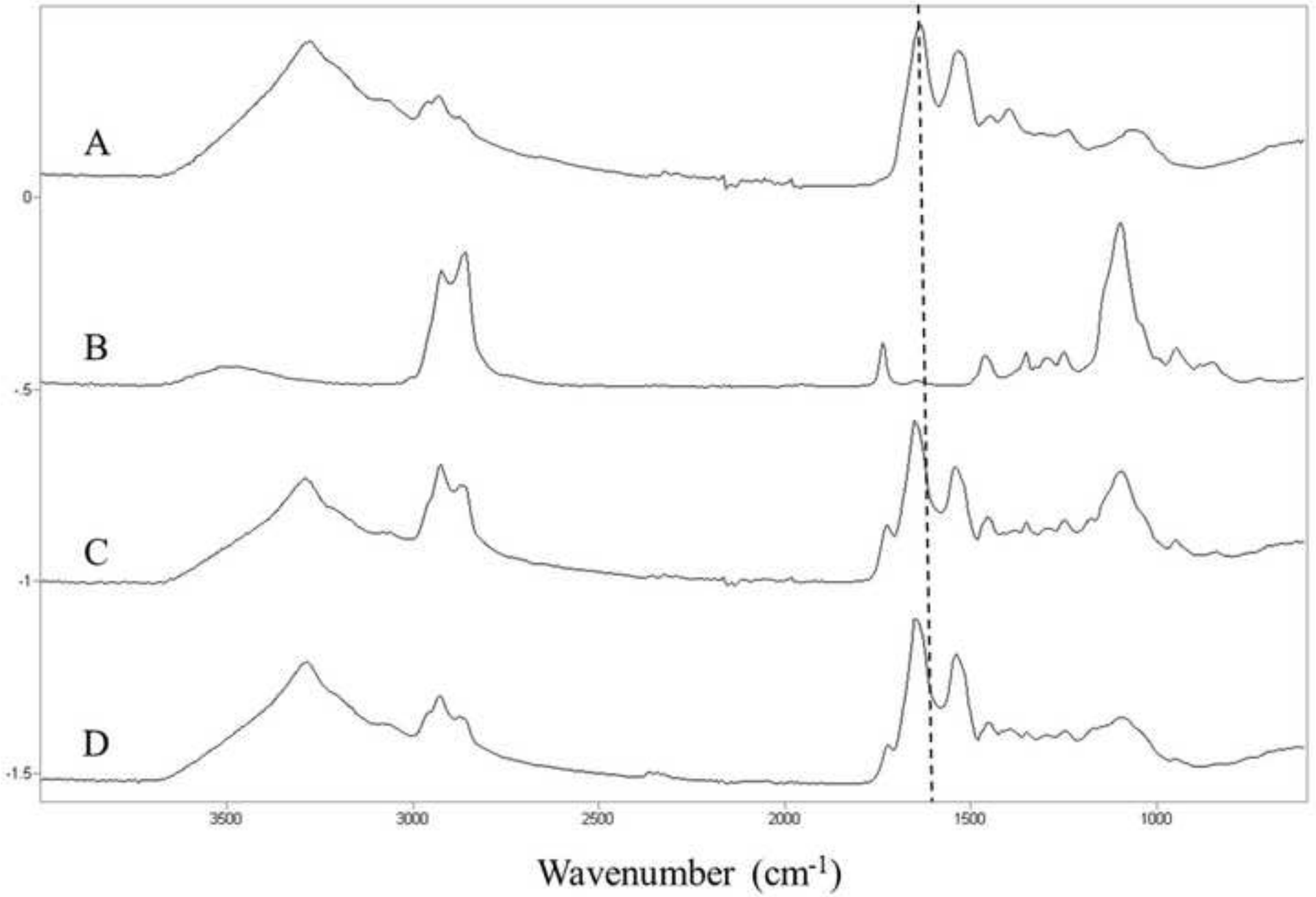

Table 1

Table 1. Effect of pH and temperature on the amaranth protein isolate solution properties and electrospun structures obtained thereof.

Solvent	%API	Conductivity (µS)	Surface Tension (mN/m)	Viscosity (cP)	Morphology	Diameter (nm)
Non-heated acetic acid solution (pH 2)	5	1575	33.7 ± 0.4^{a}	47.9 ± 6.4^{a}	-	-
Heated acetic acid solution (pH 2)	5	1706	29.9 ± 0.2^{b}	56.5 ± 8.9^{a}	Nanoparticles	569.3 ± 182.7^{a}
Non-heated NaOH 0.01M solution (pH 12)	15	4020	38.9 ± 0.5^{c}	8.5 ± 5.3^{b}	Nanoparticles	267.8 ± 82.7^{b}
Heated NaOH 0.01M solution (pH 12)	15	3610	39.8 ± 0.6^{c}	21.3 ± 3.5^{b}	Nanoparticles	169.3 ± 109.9^{c}

a-c different superscripts within the same column indicate significant differences among samples ($p<0.05$).

Table 2

Table 2. Effect of type of solvent and protein concentration on the API solution properties and electrospun structures obtained thereof.

Solvent	% API	Conductivity (µS)	Surface Tension (mN/m)	Viscosity (cP)	Morphology	Diameter (nm)
HFIP	5%	47	18.3 ± 0.2^{a}	47.2 ± 1.1^{a}	Beaded fibers	1961.5 ± 996.7^{a}
	8%	65	18.7 ± 0.3^{ab}	90.5 ± 1.6^{b}	Fibers	389.3 ± 114.5^{b}
	10%	101	19.3 ± 0.5^{b}	166.1 ± 3.8^{c}	Fibers	-
Formic acid	8%	5950	29.9 ± 0.2^{c}	92.5 ± 9.4^{b}	Beads	1375.8 ± 543.5^{c}
	10%	6820	29.3 ± 0.4^{c}	110.3 ± 5.8^{d}	Beads-fibers	1387.6 ± 357.1^{c}
	20%	8350	29.4 ± 0.2^{c}	136.6 ± 4.5^{e}	-	-

The a-e different superscripts within the same column indicate significant differences among samples ($p<0.05$).

Table 3

Table 3. Effect of surfactant and mercaptoethanol (2-ME) addition on the API-containing formic acid solution properties and electrospun structures obtained thereof.

Solvent + additive	%API	Conductivity (µS)	Surface Tension (mN/m)	Viscosity (cP)	Morphology	Diameter (nm)
Formic acid + 10% Tween80	10	5540	31.3 ± 0.1^{a}	118.9 ± 2.3^{a}	Beads	219.7 ± 86.2^{a}
Formic acid + 20% Tween80	10	5440	30.2 ± 0.4^{b}	119.5 ± 8.8^{a}	Beads	369.3 ± 159.9^{b}
Formic acid + 20% 2-ME	10	5550	30.1 ± 0.1^{b}	108.2 ± 4.9^{a}	Beads	-
Formic acid + 20% 2-ME + 15% Tween80	10	5310	30.6 ± 0.2^{b}	120.9 ± 3.4^{a}	Beads	738.5 ± 419.1^{c}

a-c different superscripts within the same column indicate significant differences among samples ($p<0.05$).

HIGHLIGHTS

- Amaranth protein isolate (API) ultrathin structures were developed by electrospinning
- The effects of pH, solvent and surfactants on morphology and molecular order were studied
- Morphology of electrospun structures was mainly affected by the solution properties
- Surfactant addition improved spinnability and morphology of API ultrathin structures

*Graphical Abstract (for review)

Click here to download high resolution image